Artificial Potential Field Approach to Path Tracking for a Non-Holonomic Mobile Robot

Mathias Jesper Sørensen

Department of Control Engineering
Institute of Electronic Systems
Aalborg University, Denmark
Email: mjs@control.auc.dk

***Abstract*— This paper introduces a novel path tracking controller for an over-actuated robotic vehicle moving in an agricultural field. The vehicle itself is a four wheel steered, four wheel driven vehicle subject to the two non-holonomic constraints of free rolling and non-slipping wheels. A dynamic model of the vehicle is developed and used, together with an artificial potential field method, to synthesize a path tracking controller. The controller drives the vehicle to its destination way-point while avoiding crossing obstacles, e. g. crop rows. One of the key features of the controller is a novel method of relating artificial forces with the drive torques of the vehicle.**

I. Introduction

Throughout modern history agricultural research has been, and still is, an area of large economic, environmental and political interests and with the introduction of robotics we are seeing innovative new tools for increasing the size and quality of agricultural outputs.

The work presented in this paper is an offspring of the interdisciplinary research project *Autonomous Platform and Information system for registration of crops and weeds* (API), which is a joint research effort between Aalborg University, The Danish Institute of Agricultural Sciences, The Royal Veterinary and Agricultural University, and a number of private investing companies.

The goal of the API project is to develop a system for crop and weed registration, and apply it to precision farming in agricultures with high profit crops. The registration consists of close range vision based collection and interpretation of crop and weed data, both present and historical. Using this information, the farmer is able to direct his farming effort (watering, weeding, fertilizing, spraying etc.) toward individual plants or patches of plants and hereby gain a number of advantages, such as

- Less use of fertilizers and chemicals
- Better crop quality
- Less strain on the field

The API system is comprised of two distinct segments

1) One or more small *Autonomous Vehicles* (AVs), whose purpose is to traverse the field along rows of crops and collect visual data from it.
2) The *Base Station*, whose purpose is to interpret the data gathered from the AVs and serve it to the farmer.

This paper focuses on the AV segment alone and in particular the navigation and control of this vehicle. A picture of the AV is shown in figure 1.

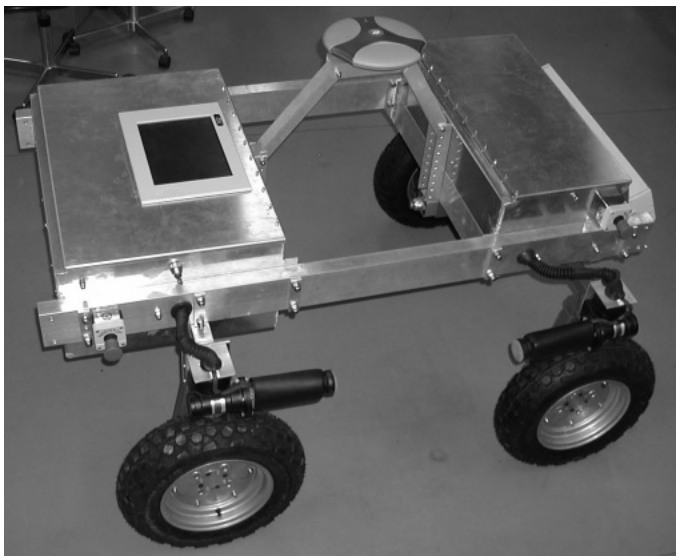

Fig. 1. The *Autonomous Vehicle*.

The wheel configuration of the AV differs from most other small vehicles, in that it is possible to steer and drive all of its four wheels individually. This gives the AV a large degree of mobility and enables it to perform sophisticated maneuvers, such as sideways driving and rotation around any point. The AV is equipped with a range of sensors for position and attitude estimation; A Differential GPS receiver, a magnetometer, a one axis fiber-optic gyro, a two axes tilt sensor, one encoder in each of the four steering actuators and one odometer in each of the four driving actuators. The AV is also equipped with a vision based row sensor, which can measure a relative position and direction of a crop row in front of the vehicle. This local information is very useful, since one of the design goals of the control strategy is to enable the AV to drive through a field without crossing crop rows.

As mentioned earlier the AV is supposed to traverse a field of row crops and collect visual data from it. The AV receives a discrete set of way points, in global coordinates,

at which a high resolution photo of the field must be taken. The problem at hand is to somehow drive the AV toward the next way point without crossing any crop rows under the following assumptions: First, the next way point is situated further down, but not necessarily on, the same crop row as the AV is currently moving along, unless the AV has reached the end of the field. In this case the next way point will lie near a crop row to the left or right of the AV. Second, no knowledge of the absolute position of the rows is known, only the relative position and orientation directly in front of the AV, given by the output from the row sensor.

A prerequisite for the control strategy proposed in this paper is that a dynamic model of the AV is known. A generic model of non-holonomic wheeled vehicles has already been introduced in [1] and adapted to the AV in [2] and [3]. [1]-[3] also introduced a trajectory tracking controller based on an exact linearizing state feedback of the highly nonlinear model. One major problem with this controller was that the full reference trajectory to be tracked had to be known in advance. Apart from this, there was also some minor problems with a singularity in the linearizing feedback at zero velocity. The strategy proposed in this paper does not involve any linearization of the model and the aforementioned singularity is no longer an issue. Also, the controller solves the problem of unknown trajectories by linking a very intuitive *artificial potential field* (APF) method directly together with the vehicle dynamics. The APF method has been used extensively in many different varieties for robotic path planning because of its simplicity [4], [5], but has also been criticized for having a number of inherent shortcomings [6], such as local trap situations and oscillations in narrow passages. None of these problems appear to have any relevance on the API system, though. The proposed controller uses an APF to generate an artificial force that would pull a free floating object toward the next way point and at the same time toward the center of the current crop row. The idea is then to steer the four wheels of the AV in such a way that the drive motors can generate torques which, when mapped onto the center of mass of the AV, are equivalent to the desired artificial force.

A dynamic model of the AV is briefly described in section II. Section III-IV describes the APF and the controller, and section V presents simulations of the closed loop system. The construction of the AV is not yet completed and hence no physical experiments have been executed.

II. Dynamic Model

The following section gives an overview of the derivation of a dynamic model of the AV. For a more in depth discussion of the model please refer to [1], [2] and [3].

A. Vehicle Definition

The AV consists of a rigid rectangular body frame and four wheels. The wheels are placed at the four corners of the vehicle and are all both steerable and drivable. The vehicle is driving in the horizontal plane and hence the position and rotation of the vehicle frame can be described by the triplet $\chi = [x\ y\ \theta]^T$, as defined in figure 2.

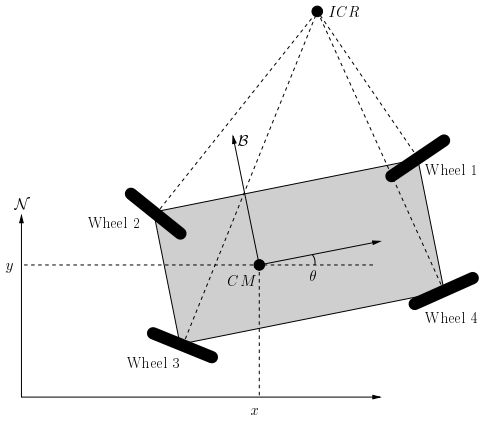

Fig. 2. Definition of the vehicle body frame coordinates. $[x\ y]^T$ are the position of the vehicle Center of Mass in the inertial coordinate frame $\mathcal{N}$. θ is the rotation of the vehicle coordinate frame $\mathcal{B}$ relative to the $\mathcal{N}$-frame.

Before proceeding, the parameters and coordinates associated with each wheel need to be defined, see figure 3.

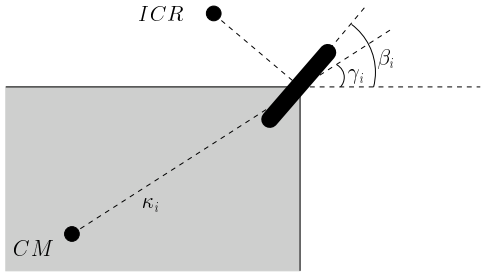

Fig. 3. Definition of parameters and coordinates related to the i'th wheel. κ_i and γ_i defines the fixed polar position of the wheel in the $\mathcal{B}$-frame, whereas β_i defines the horizontal rotation (or steering angle) of the i'th wheel itself.

The figures also defines the *Instantaneous Center of Rotation* (ICR). This point lies at the intersection of each of the four lines passing through the center of the corresponding wheel, perpendicular to the orientation of the wheel. Only two lines are needed to define an ICR, but only when all four lines intersect at a single point is the ICR defined uniquely. A unique ICR is a prerequisite for upholding the constraint of pure rolling. From now on β_3 and β_4 will therefore be determined by functions of β_1 and β_2

$$\beta_3 = \arctan\left(\frac{L\cos\beta_1\sin\beta_2}{W\sin(\beta_1-\beta_2)+L\cos\beta_1\cos\beta_2}\right)$$

and

$$\beta_4 = \arctan\left(\frac{L\sin\beta_1\cos\beta_2}{W\sin(\beta_1-\beta_2)+L\cos\beta_1\cos\beta_2}\right)$$

L and W are the length and width of the vehicle respectively. It is worth noting from these equations that there is a problem when $\beta_1 = \pm\beta_2 = \pm\pi/2$. In this case the ICR lies somewhere on the line passing through the centers of wheel 1 and 2, but it is not possible to determine exactly where based on β_1 and

β_2 alone. This is remedied by restricting the two wheel angles to lie in the open interval $\beta_1, \beta_2 \in]-\frac{\pi}{2}, \frac{\pi}{2}[$.

B. Non-holonomic Constraints

The AV is subject to the non-holonomic constraints of pure rolling and non-slipping wheels. That is, the centers of the wheels are not allowed to skid sideways, nor are they allowed to slip.

The constraint of pure rolling is described mathematically by

$$\mathbf{C}(\beta)\mathbf{R}(\theta)\dot{\chi} = \mathbf{0} \tag{1}$$

with rotation matrix

$$\mathbf{R}(\theta) = \begin{bmatrix} \cos\theta & \sin\theta & 0 \\ -\sin\theta & \cos\theta & 0 \\ 0 & 0 & 1 \end{bmatrix}$$

and projection matrix

$$\mathbf{C}(\beta) = \begin{bmatrix} -\sin\beta_1 & \cos\beta_1 & \kappa_1\cos(\beta_1-\gamma_1) \\ -\sin\beta_2 & \cos\beta_2 & \kappa_2\cos(\beta_2-\gamma_2) \\ -\sin\beta_3 & \cos\beta_3 & \kappa_3\cos(\beta_3-\gamma_3) \\ -\sin\beta_4 & \cos\beta_4 & \kappa_4\cos(\beta_4-\gamma_4) \end{bmatrix}$$

The left side of (1) is a four dimensional vector describing the sideways velocities of the four wheel centers. In a pure rolling motion there must be no sideways movement of the wheels and hence the zero vector on the right side.

The constraint of non-slipping is described by

$$\mathbf{J}_1(\beta)\mathbf{R}(\theta)\dot{\chi} = \mathbf{J}_2\dot{\phi} \tag{2}$$

with projection matrix

$$\mathbf{J}_1(\beta) = \begin{bmatrix} \cos\beta_1 & \sin\beta_1 & \kappa_1\sin(\beta_1-\gamma_1) \\ \cos\beta_2 & \sin\beta_2 & \kappa_2\sin(\beta_2-\gamma_2) \\ \cos\beta_3 & \sin\beta_3 & \kappa_3\sin(\beta_3-\gamma_3) \\ \cos\beta_4 & \sin\beta_4 & \kappa_4\sin(\beta_4-\gamma_4) \end{bmatrix}$$

and radii matrix

$$\mathbf{J}_2 = \begin{bmatrix} R_w & 0 & 0 & 0 \\ 0 & R_w & 0 & 0 \\ 0 & 0 & R_w & 0 \\ 0 & 0 & 0 & R_w \end{bmatrix}$$

The left side of (2) describes the forward velocities of the wheel centers. If the wheels do not slip, then the velocities must equal the rotational velocities $\dot{\phi}$ of the wheels multiplied with their radii $\mathbf{J}_2$.

C. Kinematics

From (1) we see that the constraint implies that the rotated velocity vector $\mathbf{R}(\theta)\dot{\chi}$ lies in the null-space of $\mathbf{C}(\beta)$. If we can find a set of vectors, that spans this null-space, then there exists a signal η such that

$$\mathbf{R}(\theta)\dot{\chi} = \Sigma(\beta)\eta \tag{3}$$

where

$$span[col[\Sigma(\beta)]] = null(\mathbf{C}_1(\beta))$$

One possible $\Sigma(\beta)$ is

$$\Sigma(\beta) = \begin{bmatrix} \cos\beta_2\kappa_1\cos(\beta_1-\gamma_1) - \cos\beta_1\kappa_2\cos(\beta_2-\gamma_2) \\ \sin\beta_2\kappa_1\cos(\beta_1-\gamma_1) - \sin\beta_1\kappa_2\cos(\beta_2-\gamma_2) \\ \sin(\beta_1-\beta_2) \end{bmatrix}$$

The dimension of η is determined by the dimension of $null(\mathbf{C}_1(\beta))$, i.e. η is a scalar. We are now left with the following kinematic relations

$$\dot{\chi} = \mathbf{R}^T(\theta)\Sigma(\beta)\eta \tag{4}$$

$$\dot{\phi} = \mathbf{J}_2^{-1}\mathbf{J}_1(\beta)\Sigma(\beta)\eta \tag{5}$$

$$[\dot{\beta}_1\ \dot{\beta}_2]^T = \zeta \tag{6}$$

with $\eta \in \mathbb{R}$ and $\zeta \in \mathbb{R}^2$ being the inputs to the kinematic model.

D. Dynamics

The equations (4)-(5) are difficult to use in a controller directly. η is not easy to measure and it is not a direct physical input to the system. A dynamic relation that connects the input torques of the wheels to η is needed. The dynamics of ζ will not be considered further, as it is assumed that it is possible to control the wheels based only on the kinematic relation of (6). This assumption is valid if the dominating dynamics are determined by the movement of the vehicle body and not by the turning of the wheels.

The dynamics of η is derived using the Lagrange formalism on differential geometry [9]. The two Lagrange equations governing the dynamics of the generalized coordinates χ and ϕ are

$$\frac{d}{dt}\left(\frac{\partial T}{\partial \dot{\chi}}\right) - \frac{\partial T}{\partial \chi} = \mathbf{R}^T(\theta)\mathbf{J}_1^T(\beta)\lambda_1 + \mathbf{R}^T(\theta)\mathbf{C}_1^T(\beta)\lambda_2 \tag{7}$$

$$\frac{d}{dt}\left(\frac{\partial T}{\partial \dot{\phi}}\right) - \frac{\partial T}{\partial \phi} = -\mathbf{J}_2^T\lambda_1 + \tau_\phi \tag{8}$$

$\lambda_1, \lambda_2 \in \mathbb{R}^4$ are the Lagrange multipliers, which are derived from the non-holonomic constraints of (1) and (2). The torque vector $\tau_\phi \in \mathbb{R}^4$ is the input to the four drive motors and T is the total kinetic energy of the AV

$$T = \frac{1}{2}\dot{\chi}^T\mathbf{R}^T(\theta)\mathbf{M}\mathbf{R}(\theta)\dot{\chi} + \frac{1}{2}\dot{\phi}^T\mathbf{I}_w\dot{\phi} \tag{9}$$

where $\mathbf{M}$ is a constant symmetric positive definite matrix derived from the wheel masses and the mass and moment of inertia of the vehicle body itself. $\mathbf{I}_w$ is a diagonal positive definite matrix derived from the moments of inertia of the wheels. After some manipulation of the Lagrange equations the final dynamic equation emerges

$$\begin{aligned} &\Sigma^T(\beta)\left[\mathbf{M} + \mathbf{E}^T(\beta)\mathbf{I}_w\mathbf{E}(\beta)\right]\Sigma(\beta)\dot{\eta} \\ &\quad + \Sigma^T(\beta)\left[\mathbf{M} + \mathbf{E}^T(\beta)\mathbf{I}_w\mathbf{E}(\beta)\right]\Gamma(\beta,\eta)\zeta \\ &\quad = \Sigma^T(\beta)\mathbf{E}^T(\beta)\tau_\phi \end{aligned} \tag{10}$$

where $\mathbf{E}(\beta) = \mathbf{J}_2^{-1}\mathbf{J}_1(\beta)$ and $\Gamma(\beta,\eta)\zeta = \dot{\Sigma}(\beta)\eta$.

The dynamic equation (10) and the two kinematic relations in (4) and (6) constitutes the complete nonlinear model of the

vehicle. The kinematics and dynamics of ϕ have been left out of the final model, since only the control of χ and β will be of interest in the following.

III. Artificial Potential Field

Artificial potential field (APF) methods have been used extensively in robot path planning and obstacle avoidance, mainly because of its elegance and intuitive simplicity.

The basic idea of the method is to generate an artificial potential field map $\Psi(\cdot)$ in the environment surrounding the robot. The most common way to build the map is to let the reference path or point represent a potential that decreases, when the robot approaches the reference. Obstacles on the other hand represents increasing potentials when the robot gets closer. In other words the reference represents valleys and ravines, whereas obstacles represents mountains and ridges on the potential map. To reach the reference and avoid the obstacles, the robot should then follow the path with the least potential. An obvious way would be to use the method of steepest descent and move in the direction of the gradient $-\nabla\Psi(\cdot)$. The gradient can be seen as an artificial force that pushes the robot toward a steady state, i.e. a minimum in the potential field.

In the case of the AV there is a known reference way-point and a partially unknown reference path, which should be along a crop row. A potential difference between the way-point and the position of the AV can easily be defined. For example by using the square of the distance from the current position of the AV to the way-point

$$\begin{aligned} \Psi_{wp}(\chi) &= \frac{1}{2}(\chi - \chi_{wp})^T \mathbf{K}_{wp}(\chi - \chi_{wp}) \\ \Rightarrow \qquad \nabla_\chi \Psi_{wp}(\chi) &= \mathbf{K}_{wp}(\chi - \chi_{wp}) \end{aligned}$$

the diagonal matrix $\mathbf{K}_{wp}$ is a design parameter, with which the amplitude of the potential field can be scaled. The reference path toward the way-point is only known by a distance to, and an orientation of a nearby crop row relative to the AV. Under the assumption, that the crop row is approximately linear in the vicinity of the AV, the position and orientation of the crop row at the point closest to χ can be calculated. This will be denoted χ_{cr}. If the AV is to track the crop row, then the squared distance between χ and χ_{cr} should approach zero and a potential difference associated with the crop row would be

$$\begin{aligned} \Psi_{cr}(\chi) &= \frac{1}{2}(\chi - \chi_{cr})^T \mathbf{K}_{cr}(\chi - \chi_{cr}) \\ \Rightarrow \qquad \nabla_\chi \Psi_{cr}(\chi) &= \mathbf{K}_{cr}(\chi - \chi_{cr}) \end{aligned}$$

where another design parameter $\mathbf{K}_{cr}$ has been introduced.

At first glance this APF seems to be a reasonable guess for a APF, that would drive the AV to the way-point, if the gradient $\mathbf{F}_T(\chi) = -\nabla_\chi \Psi_{wp}(\chi) - \nabla_\chi \Psi_{cr}(\chi)$ is used as the driving force. This is visualized in figure 4 at three different points. Note that the orientation of the AV is left out for readability.

There is a problem, though. Only the 'potential energy' has been discussed, and nothing has been said about the kinetic

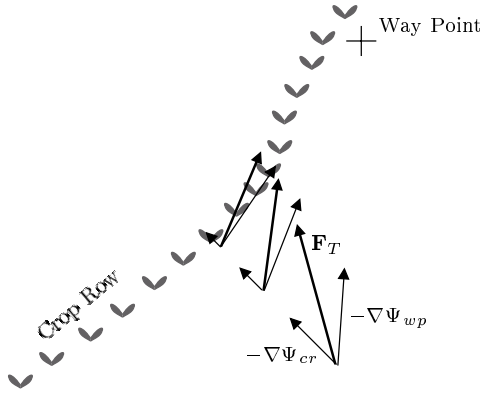

Fig. 4. Different gradients derived from the artificial potential field.

energy of the vehicle. The build up of kinetic energy will surely make the AV overshoot the way-point, so the kinetic energy has to be included somehow to make sure that the total energy of the vehicle is zero at the way-point. The kinetic energy has already been defined in (9), but this is a rather complex term. To keep it simple the following approximated kinetic energy equation is used instead

$$\begin{aligned} \Psi_T(\dot{\chi}) &= \frac{1}{2}\dot{\chi}^T \mathbf{K}_T \dot{\chi} \\ \Rightarrow \qquad \nabla_{\dot{\chi}} \Psi_T(\dot{\chi}) &= \mathbf{K}_T \dot{\chi} \end{aligned}$$

This also gives the designer more freedom to scale the effects of the different energy terms by choosing appropriate values of $\mathbf{K}_{wp}$, $\mathbf{K}_{cr}$ and $\mathbf{K}_T$.

The final driving force becomes

$$\begin{aligned} \mathbf{F}_T(\chi, \dot{\chi}) &= -\nabla_\chi \Psi_{wp}(\chi) - \nabla_\chi \Psi_{cr}(\chi) - \nabla_{\dot{\chi}} \Psi_T(\dot{\chi}) \\ &= \mathbf{K}_{wp}(\chi_{wp} - \chi) + \mathbf{K}_{cr}(\chi_{cr} - \chi) - \mathbf{K}_T \dot{\chi} \end{aligned} \tag{11}$$

which closely resembles the feedback of an ordinary PD-controller.

IV. Controller Synthesis

The artificial force $\mathbf{F}_T(\chi, \dot{\chi}) = [F_x \ F_y \ \tau_\theta]^T$ describes the translational force $[F_x \ F_y]^T$ and rotational torque τ_θ needed to drive the AV toward the next way-point along a crop row. If the AV had been an omni-directional vehicle, then $\mathbf{F}_T(\chi, \dot{\chi})$ could be applied directly through the driving actuators, and the vehicle would eventually reach the way-point. But the AV is subject to kinematic constraints, which makes a direct application of $\mathbf{F}_T(\chi, \dot{\chi})$ difficult. The only direct applicable forces/torques τ_ϕ are through the four drive motors, along the direction of each wheel.

The controller proposed in this section uses the assumption that the wheels can always be oriented in such a way that it is possible to apply a force through τ_ϕ that corresponds to the outside artificial force $\mathbf{F}_T(\chi, \dot{\chi})$. The idea is to map the artificial force onto the centers of the wheels and then turn the wheels, so that they point in the same direction as the mapped force. With this configuration the artificial force only exerts a force in the forward direction of each wheel and it is

possible to imitate this force completely with the use of the drive motors. The last task is then to find the relation between $\mathbf{F}_T(\chi, \dot{\chi})$ and τ_ϕ.

A. Wheel Steering

It is assumed that the center of mass of the AV is approximately equal to the geometric center of the vehicle. In this case the four drive motors contribute equally to the total force exerted on the vehicle.

Figure 5 shows the mapping of the elements of $\mathbf{F}_T(\chi, \dot{\chi})$ onto the i'th wheel where

$$|F_i(\tau_\theta)| = \frac{\tau_\phi}{\kappa_i} \qquad \angle F_i(\tau_\theta) = \theta + \gamma_i + \frac{\pi}{2}$$

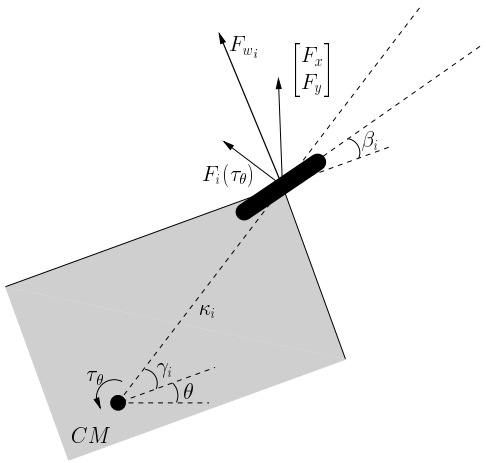

Fig. 5. Artificial forces acting wheel i.

The vector $[F_x \ F_y]^T$ is the same for all four wheels. $F_i(\tau_\theta)$ on the other hand, which is the force exerted on the wheel by the turn torque τ_θ, will differ if $\tau_\theta \neq 0$. $F_{w_i} = [F_x \ F_y]^T + F_i(\tau_\theta)$ is the total artificial force exerted on wheel i and to avoid any sideways forces acting on the wheels, the reference to the wheel must be

$$\beta_{i_{ref}} = \angle F_{w_i} - \theta$$

Note that the amplitude of F_{w_i} is not scaled down to size, because only the angle of the resulting force is of interest.

How one should design a controller to follow the reference depends on the steering actuator. The physical actuators on the AV are fast turning DC-motors with negligible dynamics and a very simple positioning controller with feedback gain K_β should be sufficient

$$\zeta_i = K_\beta \left((\angle F_{i_w} - \theta) - \beta_i \right)$$

B. Force Equivalence

Now that the wheel steering has been dealt with, the last step in the controller synthesis is to find the drive torque vector τ_ϕ, which will be equivalent to the known artificial force $\mathbf{F}_T(\chi, \dot{\chi})$. This is done by comparing two models. One is the original model derived earlier, where the AV is driven by τ_ϕ, and the other is a model, where the AV is driven by the artificial force $\mathbf{F}_T(\chi, \dot{\chi})$.

The original Lagrange equations of (7) and (8) resulted in the dynamic equation of (10). The *generalized force* τ_ϕ acted on the *generalized coordinates* ϕ and it was inserted accordingly in (8). If the AV is to be driven by the generalized force $\mathbf{F}_T(\chi, \dot{\chi})$ instead, then this force would act on the generalized coordinates χ and the Lagrange equations takes the form

$$\begin{aligned} \frac{d}{dt}\left(\frac{\partial T}{\partial \dot{\chi}}\right) - \frac{\partial T}{\partial \chi} &= \mathbf{R}^T(\theta)\mathbf{J}_1^T(\beta)\lambda_1 \\ &\quad + \mathbf{R}^T(\theta)\mathbf{C}_1^T(\beta)\lambda_2 + \mathbf{F}_T(\chi, \dot{\chi}) \\ \frac{d}{dt}\left(\frac{\partial T}{\partial \dot{\phi}}\right) - \frac{\partial T}{\partial \phi} &= -\mathbf{J}_2^T\lambda_1 \end{aligned}$$

These two equations leads to the slightly modified dynamic model

$$\begin{aligned} &\Sigma^T(\beta)\left[\mathbf{M} + \mathbf{E}^T(\beta)\mathbf{I}_w\mathbf{E}(\beta)\right]\Sigma(\beta)\dot{\eta} \\ &\quad + \Sigma^T(\beta)\left[\mathbf{M} + \mathbf{E}^T(\beta)\mathbf{I}_w\mathbf{E}(\beta)\right]\Gamma(\beta, \eta)\zeta \\ &\qquad = \Sigma^T(\beta)\mathbf{R}(\theta)\mathbf{F}_T(\chi, \dot{\chi}) \end{aligned} \quad (12)$$

The left side of (10) and (12) are the same and equating them yields the important relation

$$\Sigma^T(\beta)\mathbf{E}^T(\beta)\tau_\phi = \Sigma^T(\beta)\mathbf{R}(\theta)\mathbf{F}_T(\chi, \dot{\chi}) \quad (13)$$

This is a scalar equation with four unknown and therefore impossible to solve uniquely, but nothing prohibits us from distributing the wheel torques evenly by setting $\tau_\phi = \mathbf{H}\tau_s$, where $\mathbf{H} = [1 \ 1 \ 1 \ 1]^T$. Now, there is only one unknown and (13) can be solved

$$\tau_\phi = \mathbf{H}\frac{\Sigma^T(\beta)\mathbf{R}(\theta)}{\Sigma^T(\beta)\mathbf{E}^T(\beta)\mathbf{H}}\mathbf{F}_T(\chi, \dot{\chi}) \quad (14)$$

It can be shown by inspection [2] that the denominator is non-zero as long as the constraint of non-slipping wheels are not violated and both β_1 and β_2 lie in the open interval $]-\frac{\pi}{2}, \frac{\pi}{2}[$.

An analytic proof of stability and convergence will not be given in this paper, but after inspection of numerous simulations, one of which is shown in the next section, the proposed controller structure seems to be stable. It has not been possible to force it into an unstable configuration (yet), but proof of stability should be the next obvious step in an analysis of the proposed controller structure.

V. Simulation Results

Figure 6 depicts a simulation run where the AV is following two parallel crop rows. The AV starts at $\chi = [0 \ 0 \ 0]^T$ and is given a way-point (WP 1) at the end of the first row. The only information it has about the crop row is the position of the nearest point on the row and the direction of the row at this point. When it has reach WP 1, it is given two intermediate way-points (WP 2 and 3), one at a time, to help it reach the beginning of the next row. During the row change it does not receive any crop row information. When the row change is completed the AV is given it's final way-point (WP 4) at

the end of the second row. The values of the way-points are summarized in table I.

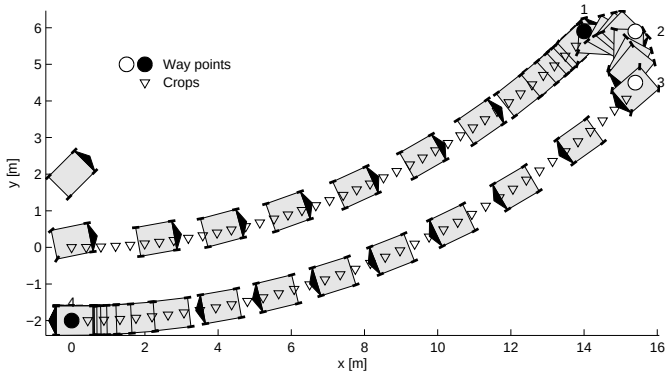

Fig. 6. Row tracking and row change.

TABLE I

WAY-POINT COORDINATES.

	x	y	θ
Initial state	0	2	$\frac{\pi}{4}$
WP 1	14	5.9	$\frac{1}{4}\pi$
WP 2 (intermediate)	15.4	5.9	$-\frac{1}{4}\pi$
WP 3 (intermediate)	15.4	4.5	$-\frac{3}{4}\pi$
WP 4	0	-2	$-\pi$

Figure 7 shows the input and error signals for this simulation. $error_p$ is the least square distance between the AV and the crop row and $error_\theta$ is the orientation difference between the AV and the crop row. Between $t \approx 25$ and $t \approx 41$ the AV is changing rows and data from the row sensor is turned off. The error signals are not defined in this interval, hence the black boxes.

The curvature of the crop rows of figure 6 is rather large compared to an average field. The potential of the target way-points will always try to drive the AV in a straight line toward the next way-point, and the large curvature means that the AV will be forced away from the crop row at the beginning of the row. The error is hence larger in the beginning of the simulation and again after $t \approx 41$, where the AV hits the second crop row. More important is the fact that the controller is still able to keep the wheels from touching the crops, despite the error. In a field with straighter crop rows the errors are reduced considerably.

VI. CONCLUSION

In this paper we considered the path tracking problem of a four wheel steered, four wheel driven autonomous vehicle or AV, subject to non-holonomic constraints. The mission of the AV is to traverse a field of crop rows and gather visual data from it. The AV has to drive through the field along the crop rows, doing as little damage to the crops as possible. At the same time it has to reach certain way-points given to it from a higher level in the navigation structure. The only information

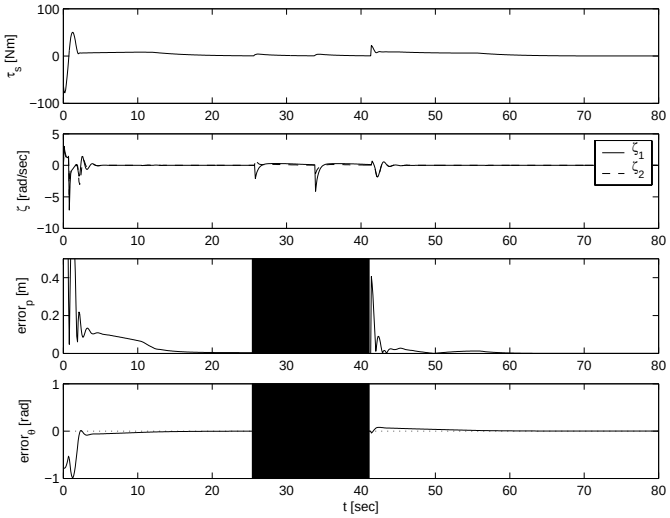

Fig. 7. Input and error signals from the simulation run of figure 6.

the AV has of the field is the absolute position of the next way-point and the relative distance to and orientation of the nearest crop row.

A path tracking control strategy was proposed based on an artificial potential field together with a dynamic model of the AV. The proposed controller had one distinct advantages as opposed to typical controllers based on linearizing feedback. The method of linking the theory of artificial potential fields directly to the dynamics of the vehicle made the controller very intuitive and easy to grasp. As seen in a simulation of the controller, it effectively guided the AV toward the next way-point without damaging the crops.

REFERENCES

[1] B. Thuilot, B. d'Andréa Novel, and A. Micaelli, "Modeling and feedback control of mobile robots equipped with several steering wheels," *IEEE Trans. Robot. Automat.*, vol. 12, no. 3, pp. 375–390, June 1996.

[2] M. J. Sørensen, "Modeling and control of wheeled farming robot," Master's thesis, Aalborg University, Department of Control Engineering, 2002, http://www.control.auc.dk/˜mjs/publications/sorensen_01_2002.pdf.

[3] J. D. Bendtsen, P. Andersen, and T. S. Pedersen, "Robust feedback linearization-based control design for a wheeled mobile robot," in *Proceedings of the 6th International Symposium on Advanced Vehicle Control*, 2002.

[4] M. D. Adams, "High speed target pursuit and asymptotic stability in mobile robotics," *IEEE Trans. Robot. Automat.*, vol. 15, no. 2, pp. 230–237, April 1999.

[5] S. S. Ge and Y. J. Cui, "New potential functions for mobile robot path planning," *IEEE Trans. Robot. Automat.*, vol. 16, no. 5, pp. 615–620, October 2000.

[6] Y. Koren and J. Borenstein, "Potential field methods and their inherent limitations for mobile robot navigation," in *IEEE Conference on Robot. Automat.*, April 1991, pp. 1398–1404.

[7] S. Sastry, *Nonlinear Systems: Analysis, Stability and Control*. New York: Springer, 1999.

[8] B. Thuilot, B. d'Andréa Novel, and A. Micaelli, "Structural properties and classification of kinematic and dynamic models of wheeled robots," vol. 12, no. 1, pp. 47–62, February 1996.

[9] H. Goldstein, *Classical Mechanics*, 2nd ed. Addison-Wesley, 1980.

[10] H. K. Khalil, *Nonlinear Systems*, 2nd ed. Prentice Hall, 1996.